Evaluation of the Role of Specific Acidic Amino Acid Residues in Electron Transfer between the Flavodoxin and Cytochrome c_3 from *Desulfovibrio vulgaris* [Hildenborough]†

Yucheng Feng and Richard P. Swenson*

Department of Biochemistry, The Ohio State University, Columbus, Ohio 43210

Received June 30, 1997; Revised Manuscript Received August 7, 1997⊗

ABSTRACT: A hypothetical model for electron transfer complex between cytochrome c_3 and the flavodoxin from the sulfate-reducing bacteria *Desulfovibrio vulgaris* has been proposed, based on electrostatic potential field calculations and NMR data [Stewart, D. E., LeGall, J., Moura, I., Moura, J. J. G., Peck, H. D., Jr., Xavier, A. V., Weiner, P. K., & Wampler, J. E. (1988) *Biochemistry 27*, 2444−2450]. This modeled complex relies primarily on the formation of five ion pairs between lysine residues of the cytochrome and acidic residues surrounding the flavin mononucleotide cofactor of the flavodoxin. In this study, the role of several acidic residues of the flavodoxin in the formation of this complex and in electron transfer between these two proteins was evaluated. A total of 17 flavodoxin mutants were studied in which 10 acidic amino acids—Asp62, Asp63, Glu66, Asp69, Asp70, Asp95, Glu99, Asp106, Asp127, and Asp129—had been permanently neutralized either individually or in various combinations by substitution with their amide amino acid equivalent (*i.e.*, asparate to asparagine, glutamate to glutamine) through site-directed mutagenesis. The kinetic data for the transfer of electrons from reduced cytochrome c_3 to the various flavodoxin mutants do not conform well to a simple bimolecular mechanism involving the formation of an intermediate electron transfer complex. Instead, a minimal electron transfer mechanism is proposed in which an initial complex is formed that is stabilized by intermolecular electrostatic interactions but is relatively inefficient in terms of electron transfer. This step is followed by a rate-limiting reorganization of that complex leading to efficient electron transfer. The apparent rate of this reorganization step was enhanced by the disruption of the initial electrostatic interactions through the neutralization of certain acidic amino acid residues leading to faster overall observed electron transfer rates at low ionic strengths. Of the five acidic residues involved in ion pairing in the modeled complex proposed by Stewart *et al.* (1988), the kinetic data strongly implicate Asp62, Glu66, and Asp95 in the formation of the electrostatic interactions that control electron transfer. Less certainty is provided by this study for the involvement of Asp69 and Asp129, although the data do not exclude their participation. It was not possible to determine whether the modeled complex represents the optimal configuration for electron transfer obtained after the reorganization step or actually represents the initial complex. The data do provide evidence for the importance of electrostatic interactions in electron transfer between these two proteins and for the existence of alternative binding modes involving acidic residues on the surface of the flavodoxin other than those proposed in that model.

Electron transfer reactions between proteins are essential for life. Though several reactions in a living cell involving protein−protein electron transfer have been characterized, much is still unknown about this mechanism at the molecular structural level. Pelletier and Kraut (1992) recently solved the first crystal structure of an electron transfer protein pair—the cytochrome *c*−cytochrome *c* peroxidase complex. But it is unclear whether this complex represents the active form of the electron transfer complex. Most of the interactions between electron transfer proteins are based on hypothetical models (*e.g.*, Stewart *et al*., 1988; Palma *et al.*, 1994; Weber & Tollin, 1985).

One such model is the electron transfer complex between the tetraheme cytochrome c_3 and flavodoxin from sulfate-reducing bacteria such as *Desulfovibrio vulgaris*. Both are small proteins with molecular masses of 14 000 and 16 000 Da, respectively, and are involved in low-potential electron transfer reactions. The midpoint potentials of the heme groups in cytochrome c_3 range from −190 to −355 mV (Moreno *et al*., 1991). The flavodoxin from this bacterium is an acidic protein containing a tightly bound flavin mononucleotide (FMN)[1] cofactor as the only redox center, with midpoint potentials of −150 mV for the oxidized/semiquinone (ox/sq) couple and −445 mV for the semiquinone/hydroquinone (sq/hq) couple (Curley *et al.*, 1991;

† This study was supported in part by Grant GM36490 from the National Institutes of Health.

* To whom correspondence should be addressed: Department of Biochemistry, 776 Biological Sciences Bldg., The Ohio State University, 484 West 12th Ave., Columbus, OH 43210-1292. Tel 614-292-9428; Fax 614-292-6773; e-mail swenson.1@osu.edu.

⊗ Abstract published in *Advance ACS Abstracts,* October 15, 1997.

[1] Abbreviations: FMN, flavin mononucleotide; *fld*$^{+n}$, flavodoxin mutant in which *n* acidic amino acid residues had been permanently neutralized through the acid-to-amide substitution (see Table 2 for description); cyt_{ox} and cyt_{red}, oxidized and reduced forms of cytochrome c_3, respectively; ox/sq, oxidized/semiquinone; sq/hq, semiquinone/hydroquinone.

S0006-2960(97)01576-6 CCC: $14.00

Table 1: Oligonucleotide Sequences for Site-Directed Mutagenesis

mutation	oligonucleotide sequence[a]	restriction site[b]
D69N	5′-GGAATGAAGTCGTTCTGCAGTTCG-3′	*Xmn*I (+)
D70N	5′-GGAATGAAGTTGTCT*TGCAGTTCG-3′	*Pst*I (−)
D127N	5′-GGTCGCCATTGATGCGAAGACC-3′	*Cla*I (−)
D129N	5′-GCGCGGGGATTGCCATCGATGC-3′	*Mam*I (+)

[a] The underlined nucleotides are different from the wild type, and asterisk indicates the "silent" mutation introduced to eliminate restriction site. [b] Restriction sites are either created (+) or eliminated (−) as the consequence of mutation.

Swenson & Krey, 1994; Zhou & Swenson, 1995). Electron transfer involving these two proteins have been implicated in the phosphoroclastic reaction and sulfite reduction in these organisms (Moura *et al.*, 1978, 1984). The *in vitro* reconstitution of complex electron-transfer pathways involving the reduction of sulfite by molecular hydrogen and the production of hydrogen from aldehydes *via* aldehyde dehydrogenase requires the presence of both flavodoxin and cytochrome c_3 (Chen *et al*., 1993; Barata *et al*., 1993). Also, there is experimental evidence that these two proteins form binary and ternary complexes of good stability and support efficient intermolecular electron transfer, again, *in vitro* (Palma *et al*., 1994; De Francesco *et al.*, 1994). However, there is some uncertainty as to whether these proteins represent a true physiological electron transfer pair in the bacterium because flavodoxins are intracellular proteins, while the majority of the cytochrome c_3 resides in periplasm (Badziong & Thauer, 1980). Nonetheless, because of their small sizes, established crystal structures, and evidence for efficient electron transfer *in vitro*, this pair of proteins has served as a good model system for studying the intermolecular electron transfer between heme groups and flavin cofactors and for intermolecular electron transfer between heme groups (De Francesco *et al*., 1994; Cheddar *et al*., 1986).

Stewart *et al*. (1988) constructed a hypothetical model of the flavodoxin−cytochrome c_3 complex from *D. vulgaris*. They used interactive computer graphic modeling based on electrostatic potential field calculations and previous NMR experiments (Moura *et al*., 1982). A dominant feature of this model is the formation of intermolecular salt linkages between lysine residues surrounding the heme crevice of cytochrome c_3 and acidic residues surrounding the FMN of flavodoxin. When heme 1,[2] having the most basic environment of the hemes, and the FMN of the flavodoxin are brought into close proximity, five intermolecular salt linkages can be formed between lysine residues 15, 58, 60, 95, and 101 around heme 1 of the cytochrome and the acidic residues Asp62, Glu66, Asp69, Asp129, and Asp95 on flavodoxin. This low-energy configuration brings the *o*-xylene ring of the flavin and one edge of heme 1 within van der Waals contact of one another. The two groups are oriented in a parallel and nearly coplanar configuration that could allow for significant π-electron overlap, a situation likely to facilitate electron transfer. Unfavorable steric interference between the polypeptides or electrostatic charge repulsion was not observed in this model. A similar model was developed by Palma *et al*. (1994) for one of the proposed complexes between the cytochrome c_3 from *Desulfovibrio gigas* and the flavodoxin from *Desulfovibrio salexigens*. Both these complexes are very similar in general features to one developed earlier by Weber and Tollin (1985) for tuna cytochrome *c* and the *Clostridium MP* (a.k.a. *beijerinckii*) flavodoxin.

In this study, we have attempted to test the functional validity of this electrostatic model by examining the contribution of acidic residues in flavodoxin to intermolecular electron transfer. Ten acidic amino acids, Asp62, Asp63, Glu66, Asp69, Asp70, Asp95, Glu99, Asp106, Asp127, and Asp129, have been mutated to their amide equivalent (*i.e.*, asparate to asparagine, glutamate to glutamine), permanently neutralizing the residue in a structurally conservative manner. Various combinations of these individual substitutions were also generated, neutralizing up to a total of six negative charges (Zhou & Swenson, 1995). The ability to accept an electron from reduced cytochrome c_3 was investigated in all these mutants. Kinetic studies provide direct evidence for the formation of an initial complex that is stabilized by electrostatic interactions followed by complex reorganization step(s) prior to electron transfer. Different roles of these acidic residues playing in electron transfer have been interpreted.

MATERIALS AND METHODS

Materials. Carboxymethyl cation-exchange resin (CM Bio-Gel A) was purchased from Bio-Rad Laboratories. Granulated hydroxyapatite was prepared following published procedures (Mazin *et al*., 1974). Protocatechuate 3,4-dioxygenase was courtesy of Dr. David Ballou of the University of Michigan. Oligonucleotides were synthesized and desalted by Genosys Biotechnologies, Inc. Sodium dithionite was purchased from Sigma Chemical Co. All other chemicals were of analytical reagent grade.

Site-Directed Mutagenesis. All flavodoxin mutagenesis were based on a modified version of wild-type flavodoxin gene from *D. vulgaris* [Hildenborough] (NCIB 8303, ATCC 29579) (Krey *et al*., 1988). Four oligonucleotides were synthesized that introduce the substitutions D69N, D70N, D127N, and D129N. The sequence of each oligonucleotide (Table 1) was designed to either introduce or eliminate a restriction site as indicated to aid in screening. Oligonucleotide-directed mutagenesis was carried out by the Kunkel method (Kunkel, 1985) using the MutaGene *in vitro* mutagenesis kit obtained from Bio-Rad Laboratories. All other flavodoxin mutants had been prepared and characterized previously (Zhou & Swenson, 1995). Plasmids with mutations were transformed into *Escherichia coli* AG-1 or XL-1 competent cells and selected by restriction endonuclease mapping. Mutation(s) and the sequence integrity of the entire structural gene were further confirmed by the dideoxy chain-

[2] The numbering system for the heme groups in cytochrome c_3 used throughout this paper conforms to that used in the description of the X-ray crystal structure of the *D. vulgaris* [Miyazaki] protein (Higuchi *et al*., 1984). It should be noted that this system is different from that used by some authors in the description of the modeled complexes. For example, heme 1 referred to within this paper is sometimes designated as heme 4 according to the position of the cysteine ligands in the protein sequence.

termination DNA sequencing procedure (Sanger *et al*., 1977) using the Sequenase version 2.0 sequencing kit from U.S. Biochemical Corp.

Protein Purification. Recombinant wild-type and mutated flavodoxins were expressed in transformed *E. coli* and purified as described previously (Zhou & Swenson, 1995). Cytochrome c_3 was purified from fractions of crude cell extracts of *D. vulgaris* that pass through DEAE Bio-Gel A column equilibrated in 10 mM Tris-HCl, pH 7.6, by adsorption onto hydroxyapatite followed by ion-exchange chromatography on CM Bio-Gel A resin as described by Liu *et al*. (1988). The purity of the cytochrome c_3 preparation was checked by sodium dodecyl sulfate−polyacrylamide gel electrophoresis (SDS−PAGE). The identity of this protein as cytochrome c_3 was confirmed by its molecular mass as determined on a Kratos Kompact Maldi III time-of-flight mass spectrometer (observed mass = 14 121.7 Da; calculated mass = 14 121 Da) and by amino-terminal sequence analysis for the first five amino acid residues (observed sequence: NH_2-A-P-K-A-P-) using an Applied Biosystems 475A automatic sequencer. The ultraviolet−visible absorption spectra of this preparation in oxidized and reduced states are identical to published cytochrome c_3 spectra (Liu *et al.*, 1988).

Spectroscopic Measurements. Protein concentrations were determined on a Hewlett-Packard 8452A diode array spectrophotometer using extinction coefficients of 10 700 M^{-1} cm^{-1} at 460 nm or 8500 M^{-1} cm^{-1} at 378 nm for the flavodoxin (Swenson & Krey, 1994). For cytochrome c_3, an extinction coefficient of 120 000 M^{-1} cm^{-1} at the reduced α-band maximum (553 nm) was used (De Francesco *et al*., 1994). The extinction coefficient of 487 000 M^{-1} cm^{-1} at 410 nm for oxidized cytochrome c_3 was calculated for use thereafter.

Stopped-Flow Spectrophotometry and Kinetic Measurements. Electron transfer reaction time courses and kinetic constants were determined on a Hi-Tech Scientific SF-61 stopped-flow spectrophotometer specially equipped for anaerobic experiments. Anaerobiosis was achieved by flushing the stopped-flow mixing system with 20 mM sodium citrate buffer, pH 5.5, made anaerobic by bubbling with argon for at least 15 min. Residual oxygen was removed by flushing and filling the stopped-flow mixing unit with an anaerobic solution containing 1 mM protochatechuic acid solution in 20 mM sodium citrate, pH 5.5, and 2 units of protochatechuate-3,4-dioxygenase (Fujisawa & Hayaishi, 1968). After incubation overnight with this oxygen-scrubbing solution, the stopped-flow system was flushed and replaced by the anaerobic buffer to be used in the experiment, which was generally 10 mM sodium phosphate, pH 7.5, containing 1 mM EDTA. As needed, the ionic strength of this buffer was adjusted by dilution with distilled water or by addition of NaCl.

In a typical experiment, a 2 μM solution of cytochrome c_3 in 10 mM sodium phosphate, pH 7.5, containing 1 mM EDTA placed within a tanometer was made anaerobic by repeated cycles of a partial vacuum and argon flushing and reduced by adding a sufficient volume of a sodium hydrosulfite solution. The concentration of reduced cytochrome c_3 was measured by the absorbance at 553 nm. Flavodoxin solutions in the same buffer (at various concentrations from 20 to 200 μM before mixing) were also made anaerobic by vacuum and argon cycling. Tanometers containing the anaerobic cytochrome c_3 and flavodoxin solutions were loaded onto the stopped-flow instrument and used to fill the driving syringes. Solutions within the stopped-flow system were allowed to equilibrate to temperature before rapid mixing was initiated. Upon rapid mixing, absorbance changes were generally recorded at 553 nm to monitor cytochrome c_3 reoxidation resulting from electron transfer to the flavodoxin. Kinetic rate constants were obtained by interative fitting of the reaction absorbance traces using computer software provided with the stopped-flow instrument. The concentrations of cytochrome c_3 and flavodoxin reported in the results are the final concentrations after mixing or half that of the original solutions loaded in the instrument.

Computer Graphics. Surface electrostatics and molecular dipole moment calculations were performed using GRASP software (Nicholls & Honig, 1991) and visualized on the Silicon Graphics Iris workstation. Protein structures were from the Brookhaven Protein Data Bank (flavodoxin, 2fx2; cytochrome c_3, 2cym). Charges were assigned to the proteins using the AMBER partial and full charge set (Weiner *et al*., 1984) provided with the software.

RESULTS

Generation, Expression, and Characterization of Flavodoxin Mutants. According to the hypothetical model for the electron transfer complex proposed by Stewart *et al*. (1988), five acidic amino acids on the surface of the *D. vulgaris* flavodoxin form intermolecular salt linkages with five lysine residues on the surface of cytochrome c_3, generating the following pairs: D62/K15, E66/K58, D69/K60, D95/K101, and D129/K95. Of these acidic amino acids, D62, E66, and D95 are clustered within 13 Å of the N(1) atom of the FMN cofactor. In addition, several other acidic amino acids are also found near the FMN cofactor including D63, D70, E99, D106, and D127, and although not included in the molecular model, these residues could participate in forming alternative ion-pairing interactions in the electron transfer complex. In this study, putative ion-pairing interactions in this complex were disrupted by the conservative substitution of the amide equivalent for each of these 10 acidic amino acids, *i.e*., Asn for Asp and Gln for Glu. Several of these substitutions (D62N, D63N, E66Q, D95N, E99Q, and D106N) had been generated and characterized previously as part of another study (Zhou & Swenson, 1995). Four additional mutants (D69N, D70N, D127N, and D129N) were generated as part of this study, generating a total of 10 single mutants. This study also took advantage of the availability of several other mutant flavodoxin proteins previously produced and characterized that contain several combinations of double and triple acid-to-amide substitutions and others containing four, five, or six substitutions (Zhou & Swenson, 1995). The flavodoxin mutants used in this work are summarized in Table 2. All these mutants have ultraviolet−visible absorption spectra identical to that of wild type and all have an A_{274nm}/A_{458nm} ratio of about 4.2, indicative of stoichiometric binding of the FMN cofactor. The midpoint potentials for the ox/sq couple for this group of mutants are similar to that of the wild-type flavodoxin, as a group displaying an average value of −172 mV and ranging from −152 to −191 mV (Zhou & Swenson, 1995). As noted previously, correlations between the location or the number of charges neutralized and the midpoint potential

Table 2: Electron Transfer from *D. vulgaris* Cytochrome c_3 to the Wild-Type and Charge-Neutralized Flavodoxin Mutants[a]

flavodoxin	number of neutralized charges	fast phase		slow phase	
		k_{lim} (s^{-1})	K_{app} (μM)	k_{lim} (s^{-1})	K_{app} (μM)
		Temperature = 25 °C			
wild type	0	32.5 ± 0.8	5.0 ± 0.7	9.4 ± 0.1	11.8 ± 0.6
D62N[b]	1	49.7 ± 1.8	20.0 ± 2.2	14.6 ± 0.2	22.8 ± 1.0
D63N[b]	1	50.9 ± 1.2	13.5 ± 1.2	13.9 ± 1.6	24.9 ± 7.8
E66Q[b]	1	44.2 ± 0.8	14.1 ± 0.9	10.3 ± 0.3	15.5 ± 1.5
D69N	1	39.8 ± 1.4	19.0 ± 2.1	11.9 ± 1.3	31.2 ± 2.0
D70N	1	40.0 ± 0.9	18.1 ± 1.3	12.3 ± 0.2	48.7 ± 1.8
D95N[b]	1	77.0 ± 3.5	39.0 ± 4.1	20.5 ± 1.4	69.3 ± 8.4
E99Q[b]	1	31.2 ± 0.9	3.7 ± 0.9	5.4 ± 0.3	8.1 ± 2.2
D106N[b]	1	24.4 ± 0.6	2.0 ± 0.6	7.5 ± 0.2	5.1 ± 1.1
D127N	1	34.1 ± 0.6	14.8 ± 1.0	8.8 ± 0.2	21.4 ± 1.6
D129N	1	46.8 ± 1.3	22.4 ± 1.8	12.4 ± 0.5	40.2 ± 3.6
E99Q/D106N[b]	2	40.5 ± 1.4	24.0 ± 2.3	11.3 ± 1.0	39.7 ± 8.4
D95N/E99Q/D106N[b]	3	63.5 ± 2.6	16.4 ± 2.2	20.5 ± 2.3	39.3 ± 9.8
		Temperature = 10 °C			
wild type	0	19.5 ± 0.4	11.3 ± 0.4	4.4 ± 0.2	21.6 ± 3.1
D62N/E66Q[b]	2	260.1 ± 9.7	27.6 ± 2.7	18.8 ± 0.6	13.4 ± 1.5
D62N/D63N/E66Q[b]	3	276.0 ± 7.6	30.0 ± 2.1	15.5 ± 1.4	17.4 ± 5.2
D62N/D63N/E66Q/E99Q[b]	4 (fld^{+4})	262.0 ± 4.0	40.0 ± 1.4	23.6 ± 0.9	29.6 ± 2.9
D62N/D63N/E66Q/E99Q/D106N[b]	5 (fld^{+5})	398.1 ± 33.5	63.5 ± 10.3	71.2 ± 6.6	105.2 ± 15.9
D62N/D63N/E66Q/D95N/E99Q/D106N[b]	6 (fld^{+6})	592.8 ± 42.7	95.0 ± 11.2	91.9 ± 5.6	65.3 ± 7.3

[a] Reactions were performed in 10 mM sodium phosphate, pH 7.5, containing 1 mM EDTA under anaerobic conditions at either 10 or 25 °C as indicated. [b] These mutants were prepared and characterized previously (Zhou & Swenson, 1995).

for the ox/sq couple are not apparent. Also, the dissociation constant for the FMN for those mutants for which this information is available is quite similar to that for wild type. These observations suggest that any differences in electron transfer rates noted in this study are not likely to be the result of major changes in protein structure or in the binding and oxidation−reduction properties for ox/sq couple of the FMN cofactor.

Electron Transfer from Reduced Cytochrome c_3 to Oxidized Flavodoxin. Electron transfer properties between reduced cytochrome c_3 and oxidized flavodoxin were measured in a stopped-flow spectrophotometer under anaerobic conditions at 25 °C. Some of the mutants accept electrons from cytochrome c_3 very rapidly, with most of the reaction occurring within the dead time of the instrument. In these cases, the kinetic data were obtained at the lower temperature of 10 °C. The electron transfer reaction between reduced cytochrome c_3 (final concentration after mixing of 1 μM) and wild-type flavodoxin (final concentration was varied between 10 and 100 μM) was monitored by the decrease of absorbance at 553 nm (the λ_{max} of the α band for reduced cytochrome c_3). Representative traces of absorbance changes recorded after rapid mixing are shown in Figure 1. The absorbance trace at all flavodoxin concentrations attempted did not follow a simple pseudo-first-order single-exponential reaction but could be fit very well to two exponential phases. The fast phase was generally about 5 times faster than the slow phase. The ratio of the amplitude of the fast phase relative to the slow phase varied between 3:1 and 1:1 but was most often about 2:1. This ratio did not seem to depend on the nature of the mutation or the ionic strength of the solvent and may be at least in part the consequence of experimental error in data fitting, especially for the most rapid reactions. While this biphasic phenomenon could be attributed to a multistep electron transfer process, this interpretation has been excluded experimentally and instead has been attributed to the presence of two different cytochrome c_3 conformations (De Francesco *et al*., 1994). We found it reasonable to apply that explanation here to the wild-type and mutant flavodoxins studied. In order to simplify the data interpretation, the observed electron transfer rates associated with the major fast phase were for the most part considered throughout this paper. It should be noted, however, that the general conclusions obtained from this phase also apply to the data obtained from the slower phase.

The dependency of k_{obs} on the concentration of flavodoxin is nonlinear for the electron transfer reaction between cytochrome c_3 and the wild type and all mutant flavodoxins and can be fit to a two-parameter rectangular hyperbolic function (Figure 1, inset), from which can be derived the constants k_{lim}, the limiting observed rate at infinite flavodoxin concentration, and K_{app}, the apparent binding constant. A similar nonlinear dependency was observed for both the fast and slow phases. The fact that k_{obs} appears to reach a limiting rate at higher flavodoxin concentration is consistent with the formation of a complex between cytochrome c_3 and flavodoxin prior to electron transfer. The k_{lim} and K_{app} values obtained from these studies are summarized in Table 2. The reaction time course and electron transfer rates obtained for the wild-type recombinant flavodoxin were comparable to those obtained by De Francesco *et al*. (1994). The rates obtained with the D62N/E66Q, D62N/D63N/E66Q, fld^{+4}, fld^{+5}, and fld^{+6} mutants were very rapid and could only reliably be determined at the reduced temperature of 10 °C. The K_{app} values for wild type and the E99Q and D106N mutants are somewhat less reliable because of their low relative value and the inability to obtain data points at low flavodoxin concentrations while still maintaining pseudo-first-order conditions (*cf.* Figure 1A). It should be noted, however, that suitable data over the entire hyperbolic curve such as that shown for the fld^{+5} were obtained for the other mutants (Figure 1B). Also, most of the critical conclusions within this study are based on the more reliably determinable k_{lim} values.

For the sake of our initial analysis of the kinetic data, the 10 flavodoxin mutants containing individual substitutions

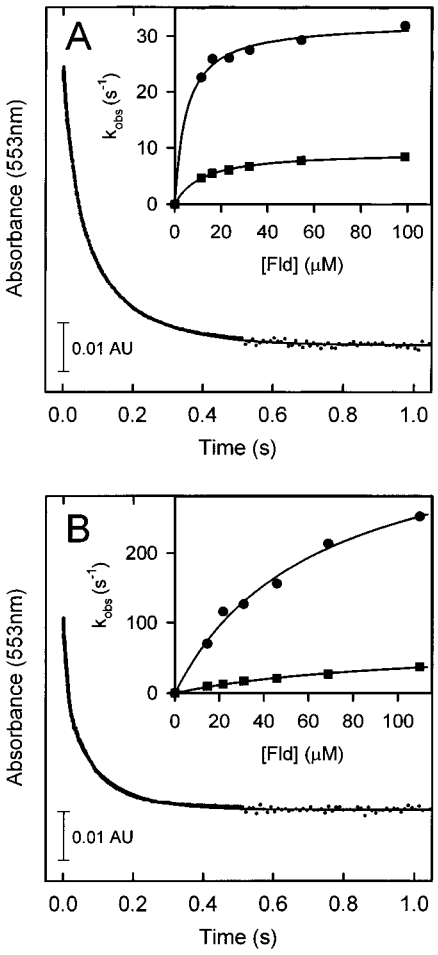

FIGURE 1: Time course of the electron transfer reaction in 10 mM sodium phosphate, pH 7.5, containing 1 mM EDTA from reduced cytochrome c_3 to flavodoxin as followed by stopped-flow spectrophotometry at 553 nm. The solid line represents the best fit of the data to a double-exponential function of the type $A = A_1e^{-k_1t} + A_2e^{-k_2t} + C$. (A) Data from mixing reduced cytochrome c_3 (1.13 μM) with wild-type flavodoxin (23.3 μM) at 25 °C. Values obtained from the fit were $A_1 = 0.0292$, $k_1 = 27.6$ s^{-1}, $A_2 = 0.0281$, and $k_2 = 6.35$ s^{-1}. (B) Kinetic trace from mixing reduced cytochrome c_3 (1.12 μM) with *fld*$^{+5}$ flavodoxin mutant (14.6 μM) at 10 °C, resulting in the following kinetic values: $A_1 = 0.0197$, $k_1 = 68.9$ s^{-1}, $A_2 = 0.0200$, and $k_2 = 9.11$ s^{-1}. Insets: Plots of k_1 (●) and k_2 (■) as a function of the flavodoxin concentration. Plots for both phases for each flavodoxin could be fit to a hyperbolic equation with $k_{lim}(1) = 32.5$ s^{-1}, $K_{app}(1) = 5.0$ μM, $k_{lim}(2) = 9.4$ s^{-1}, and $K_{app}(2) = 11.8$ μM for wild type and $k_{lim}(1) = 398$ s^{-1}, $K_{app}(1) = 64$ μM, $k_{lim}(2) = 71$ s^{-1}, and $K_{app}(2) = 105$ μM for *fld*$^{+5}$.

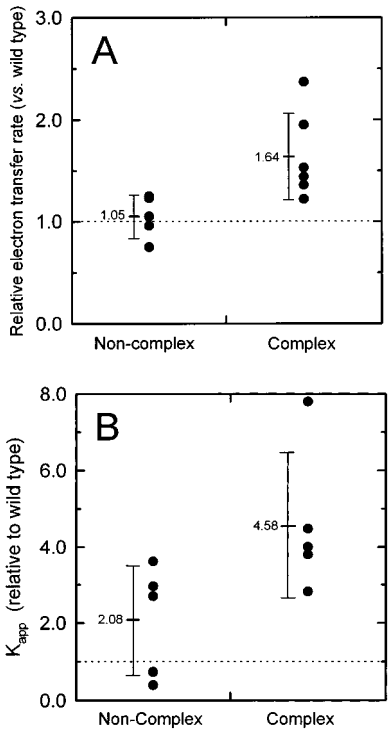

FIGURE 2: Comparison of the limiting electron transfer rates (panel A) and K_{app} values (panel B) for the singly neutralized mutants involving acidic residues not included in the modeled complex versus those that are. The bars and numerical values to the left of each group of data points represent the average ± 1 standard deviation unit for each group. The *p*-value by Student's *t*-test for the statistical difference in the averages of these two groups was calculated to be 0.02.

were divided into two groups (Figure 2A). The first group of mutants includes those acidic residues that were postulated to participate in the electron transfer complex (Stewart *et al*., 1988), including D62N, E66Q, D69N, D95N, and D129N. The second group of acidic residues not involved in that model includes D70N, E99Q, D106N, and D127N. The mutant D63N was not initially included in this analysis for reasons given below. On average, the electron transfer rates of the group not included in the complex are very similar to wild type (average relative rate = 1.05). However, the average of the rate constants of the first group is slightly higher (by approximately 60%) than the second group and may represent a statistically significant difference ($p = 0.02$, Student's *t*-test). In this analysis, the triple mutant D95N/E99Q/D106N, which contains only the one residue (D95) involved in the modeled complex, was also included in the first group and the E99Q/D106N double mutant in which none of the acidic residues was involved in the complex was included in the second group. (The inclusion of multiple mutants in this analysis will be justified below.) If these multiple mutants are omitted, a somewhat lower level of significant difference is noted ($p = 0.05$, Student's *t*-test). The mutant D63N has the highest k_{lim} of the noncomplex group. Examination of the flavodoxin structure and that of the electron transfer complex indicates that the side-chain carboxylate is very near that of Asp62, which was included in the interface of the modeled complex. It is quite plausible that Asp63 can also participate in ion pairing along with Asp62. Moving this residue into the complex-forming group increases slightly the distinction between the rate constants of these two groups. However, other evidence described below may suggest otherwise. Nonetheless, although the neutralization of those acidic residues included in the modeled complex as a group shows a slight tendency toward higher limiting k_{obs} values, the trend is not a compelling one.

Differences in the K_{app} values between the two groups were also somewhat apparent but not very compelling ($p = 0.05$, Student's *t*-test) (Figure 2B). The average K_{app} value for the group of residues involved in the modeled complex was about twice that of the noncomplex group. However, the data are skewed by the neutralizations involving Asp95, Glu99, and Asp106. The K_{app} values for the E99Q and D106N mutants (in the noncomplex group) seem to be slightly lower than for wild type and that for the D95N mutant (complex group) is significantly higher. Otherwise, all K_{app} values for the singly substituted mutants are quite similar to one another and somewhat higher than for wild type. It should be noted that it was not possible to

differentiate residues based on either the electron transfer rate or K_{app} value when each data set was examined as a single group but that the tendencies described only became apparent after dividing the singly substituted mutants into two groups on the basis of the modeled complex prior to the analysis.

The distinction between residues involved in the modeled complex and those that are not becomes much more convincing when the results for flavodoxin mutants containing multiple acid-to-amide substitutions are examined. In this regard, we were able to take advantage of several multiply mutated flavodoxins generated in a previous study (Zhou & Swenson, 1995). Some of these proteins contain substitutions involving more than one of the complex-forming acidic residues, more than one non-complex-forming residue, or mixtures of both. It should be emphasized here that it would be highly impractical to generate, purify, and analyze all possible combinations of multiple substitutions involving even the five acidic residues proposed in the modeled complex, much less all 10 involved in this study. The group of mutants studied was deemed to be reasonably representative of those residues proposed to be involved in the electron transfer complex and, as suitable controls, those thought not to be involved.

Comparisons of the maximal observed electron transfer rates of this group of mutants relative to wild type are summarized graphically in Figure 3A. The neutralization of Asp62 and Glu66 individually increased the rate constant by about 50% relative to wild type. However, k_{lim} for the double mutant D62N/E66Q increased by over 13-fold. Both residues are involved in the modeled complex. On the other hand, the double mutant E99Q/D106N displays a maximal rate constant very similar to that for wild type. Both residues are not included in the modeled complex (Stewart *et al*., 1988). When these two substitutions are combined with the neutralization of Asp95, a residue included in the modeled complex, forming the triple mutant D95N/E99Q/D106N, the rate constant is again almost 2-fold greater than wild type, similar to D95N mutation alone (Table 2). So here again, Glu99 and Asp106 do not seem to play a role, and the effect of the neutralization of an acidic residue involved in the complex (in this case Asp95) is not affected appreciably by the neutralization of non-complex-forming residues. This general phenomenon is also observed in the triple, quadruple, and quintuple mutants D62N/D63N/E66Q, D62N/D63N/E66Q/E99Q, and D62N/D63N/E66Q/E99Q/D106N, respectively. Each displays increased rate constants similar to that of the double mutant D62N/E66Q containing residues involved in the modeled complex. Thus, the additional neutralizations of residues not in the modeled complex, *i.e.* Asp63, Glu99, and Asp106, have little significant effect, although the rate was somewhat more elevated in the quintuple mutant. It is also clear from this group of mutants that the increase in relative electron transfer rates is not a general function of the number of acidic groups neutralized but more specific to the neutralization of explicit acidic residues. It is interesting to note that the side-chain carboxylate of Asp63, which was not included as one of the five acidic residues in the modeled complex, is spatially near Asp62, and conceivably could adequately substitute in the ion-pairing process. In fact, some ambivalence is noted for the homologous residues in the complex involving the closely related flavodoxin from *D. salexigens* modeled by Palma *et al.* (1994). However, it is quite evident that the D62N/E66Q double mutant behaves quite differently from the group of individually neutralized flavodoxins. One might expect that if Asp63 could effectively substitute for Asp62 in ion pairing that D62N/E66Q might behave much like E66Q, which it does not.

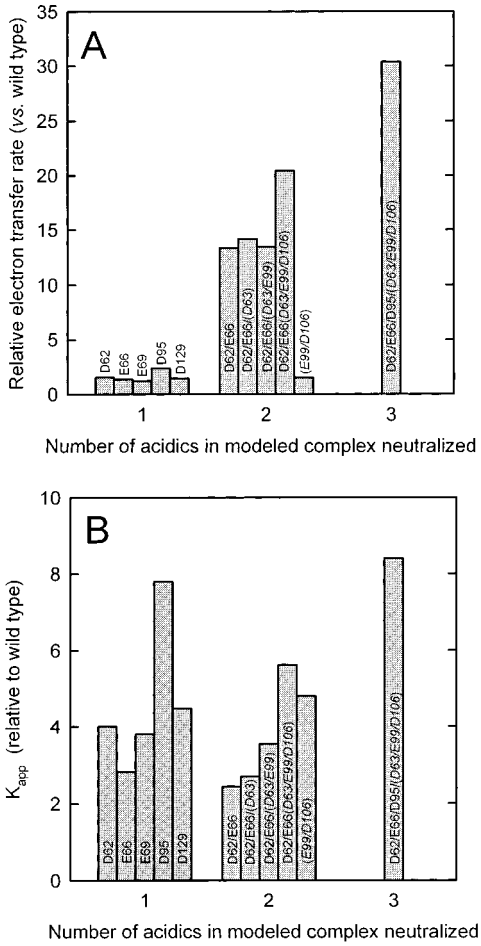

FIGURE 3: Comparison of the limiting electron transfer rates (panel A) and K_{app} values (panel B) as a function of the number of acidic residues involved in ion pairing in the modeled complex that were neutralized. Group 1 represents the results obtained for the individual independent neutralizations of the five acidic residues in the flavodoxin involved in ion pairing with lysine residues in cytochrome c_3 in the modeled complex. Group 2 represents those flavodoxin mutants in which two or more acidic residues were neutralized, of which only two—Asp62 and Glu66—are included in the modeled complex (except for the E99Q/D106N double mutant, which is included for comparison). Group 3 represents the flavodoxin mutant in which six acidic residues were neutralized, of which three—Asp62, Glu66, and Asp95—are involved in the modeled complex. The label associated with each bar identifies the residue(s) neutralized by the acid-to-amide substitution. The residue(s) included in italics within the parentheses in each case is(are) not part of the ion pairing scheme in the modeled complex but is(are) also neutralized. For example, D62/E66/(*D63*) represents the flavodoxin mutant in which Asp62, Glu66, and Asp63 have all been simultaneously substituted by their respective amide equivalents; however, only Asp62 and Glu66 but not Asp63 are postulated to form an ion pair in the complex.

Finally, relative to the quintuple mutant, the *fld*$^{+6}$ mutant contains the additional neutralization of Asp95, bringing the total neutralized complex-forming residues to three. This additional substitution resulted in a further substantial increase in the rate constant, consistent with the involvement of Asp95 in the electron transfer. It should be emphasized that these conclusions are based solely on the effects on the

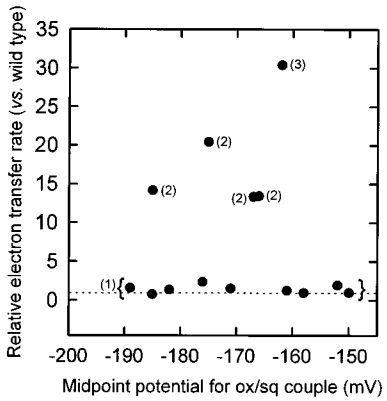

FIGURE 4: Limiting electron transfer rates (fast phase, relative to wild type) from reduced cytochrome c_3 to the flavodoxin mutant as a function of the midpoint potential for the ox/sq couple of the flavodoxin. Each point represents the results obtained for a flavodoxin mutant. With the exception of (1), the numbers in parentheses represent the number of acidic residues in that mutant that are included in ion pairing proposed in the modeled complex (not the total number neutralized). Flavodoxin mutants having a single acidic residue neutralized (irrespective of being in the complex or not), all in the group denoted (1), all cluster near a relative rate of 1 as denoted by the dashed line.

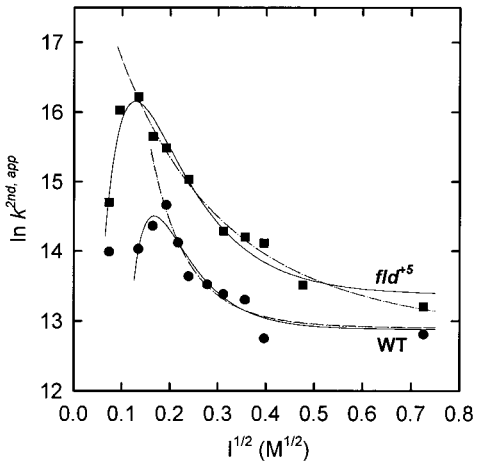

FIGURE 5: Ionic strength dependency of the natural logarithm of the apparent second-order rate constant ($k^{2nd, app}$) for the electron transfer from reduced cytochrome c_3 to the wild-type (●) and *fld*$^{+5}$ (■) flavodoxins. Each data set is fit to the Watkins "parallel plate" model (Watkins et al., 1994) using three different conditions as follows. The solid lines represent fits when both monopole−monopole and dipole−monopole interactions are included according to the equation $\ln k(I) = \ln k_\infty - V_{ii}X(I) - V_{id}Y(I)X(I)$. Parameters obtained from the fit to wild-type data are $\ln k_\infty = 13$, $V_{ii} = -120$, and $V_{id} = 280$ such that $Z_1Z_2r_{12}/D_e = -1040$ and $\rho = 35$ Å, and to *fld*$^{+5}$ data the parameters are $\ln k_\infty = 13$, $V_{ii} = -48$, and $V_{id} = 64$ such that $Z_1Z_2r_{12}/D_e = -180$ and $\rho = 22$ Å. The dashed lines represent fits to the same equation but only to the descending limbs at the higher ionic strengths. Parameters obtained from the fit to wild-type data are $\ln k_\infty = 13$, $V_{ii} = -5.6$, and $V_{id} = -25$ such that $Z_1Z_2r_{12}/D_e = -20$ and $\rho = 22$ Å, and to *fld*$^{+5}$ data the parameters are $\ln k_\infty = 13$, $V_{ii} = -5.4$, and $V_{id} = -0.99$ such that $Z_1Z_2r_{12}/D_e = -2.2$ and $\rho = 7.4$ Å. The dotted lines represent fits to the descending limbs at the higher ionic strengths when only monopole−monopole interactions are included according to the equation $\ln k(I) = \ln k_\infty - V_{ii}X(I)$. Parameters obtained from the fit to wild-type data are $\ln k_\infty = 13$ and $V_{ii} = -26$ such that $Z_1Z_2r_{12}/D_e = -150$ and $\rho = 27$ Å and to *fld*$^{+5}$ data the parameters are $\ln k_\infty = 13$ and $V_{ii} = -6.4$ such that $Z_1Z_2r_{12}/D_e = -2.9$ and $\rho = 7.8$ Å. The equations and definitions for the various parameters are as defined in Watkins *et al*. (1994) and are explained in part in the Discussion section. (Note: The dashed and dotted lines are nearly superimposed.)

neutralizations on k_{lim}. It is conceivable that a residue could play a role in complex formation without affecting the maximal rates of electron transfer. However, while overall the K_{app} values for the mutants containing multiple substitutions were higher than wild type, they are not significantly higher than for some of the single mutants. Thus, there does not appear to be a strong correlation between the K_{app} value and either the total number of acidic residues neutralized or the total number of acidic residues involved in the modeled complex (*cf*. Figure 3B).

Lack of Correlation between Electron Transfer Rate and Midpoint Potential. According to Marcus theory, the redox potential difference between the donor and acceptor is one of several factors that control the rates of electron transfer between redox centers (Marcus & Sutin, 1985). In this study, electron transfer proceeds from reduced cytochrome c_3 to oxidized flavodoxin, leading to the formation of the flavodoxin semiquinone. There is little evidence for further reduction of the flavodoxin to the fully reduced state, as is expected given the very negative midpoint potential for the sq/hq couple. The neutralization of some of the acidic residues surrounding the FMN cofactor in the flavodoxin alters the midpoint potential over a 40 mV range for the ox/sq couple, the relevant couple in these studies. These changes could affect the electron transfer rate. However, as can be seen in Figure 4, there is no meaningful correlation between the maximum electron transfer rate and the midpoint potential for the ox/sq couple of the flavodoxin mutant. The electron transfer rates were very similar for those mutants containing a single charge neutralization over the entire midpoint potential range. It is once again apparent that the rates correlate more strongly with the number of acidic residues in the modeled complex that are neutralized.

Ionic Strength Dependency. More complete ionic strength dependency studies were conducted on both the wild-type and *fld*$^{+5}$ flavodoxins. The *fld*$^{+5}$ mutant was chosen over the other mutants because several acidic residues had been neutralized and the observed electron transfer rates were more easily measured. In the case of the *fld*$^{+6}$ mutant, a significant portion of the electron transfer reaction occurred in the dead time of the stopped-flow instrument. The ionic strength of the protein solutions was adjusted by either adding NaCl into the buffer or diluting the buffer with H_2O. Experiments were carried out at 10 °C and the k_{lim} and K_{app} values were determined as before. It is well-established that if electrostatics is involved in the interaction between two proteins, ionic strength will affect the apparent second-order rate constant (Bendall, 1996). The natural logarithm of the apparent second-order rate constant was plotted as a function of the square root of ionic strength (Figure 5). For both the wild-type and *fld*$^{+5}$ flavodoxins, two phases were observed, an ascending region at low ionic strength and a descending region at high ionic strength. The lower apparent second-order rate constants at low ionic strength suggest that electrostatic interactions play a negative role in the electron transfer reaction. As the ionic strength is increased, ionic interactions begin to favor the rate of electron transfer until a maximal rate is achieved. As the ionic strength is increased further, the strength of the electrostatic interactions are weakened, leading to substantial decreases in the transfer rate. Such a phenomenon has been noted previously in other electron transfer systems [Bendall (1996) and references

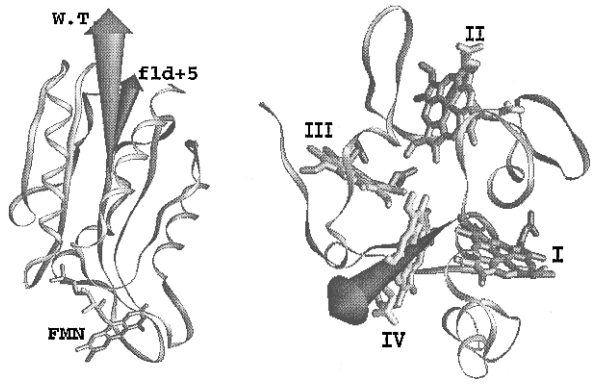

FIGURE 6: Graphical representations of the macromolecular dipole moments of the wild-type *D. vulgaris* [Hildenborough] flavodoxin, the *fld*$^{+5}$ flavodoxin mutant, and cytochrome c_3 as calculated by the molecular graphics program GRASP (Nicholls & Honig, 1991) using the AMBER partial and full charge set (Weiner *et al*., 1984) provided with the software. The heme groups in the cytochrome are numbered according to the X-ray crystal structure of the *D. vulgaris* [Miyazaki] protein (Higuchi *et al*., 1984). The vectors for the wild-type and *fld*$^{+5}$ flavodoxin mutant are superimposed on the same structure for comparison. The arrowhead points in the direction of the positive moment in each protein. The scales for the flavodoxin and cytochrome c_3 are 2.5 and 0.5 D/Å, respectively.

therein]. The mechanistic implications of these observations will be discussed in more detail in the Discussion section.

Dipole Moment Calculation. Flavodoxin and cytochrome c_3 are both proteins with asymmetric charge distributions. Flavodoxin has a net negative charge at physiological pH, and most of the acidic residues are distributed close to FMN. Cytochrome c_3 is rich in lysine residues, and has a net positive charge at physiological pH. The surface surrounding heme 1 is the most positive. Both proteins have a permanent dipole moment and this could assist in their orientation as they approach one another prior to complex formation, as has been proposed for other electron transfer systems (Koppenol & Margoliash, 1982; Margoliash & Bosshard, 1983; Roberts *et al*., 1991). The macrodipole moments of both proteins were calculated using the GRASP software program and are presented graphically in Figure 6 (Nicholls & Honig, 1991). The effects of the acid-to-amide substitutions introduced in the flavodoxin on this dipole moment were also evaluated (data not shown). As expected, the magnitude of the dipole moment of flavodoxin mutants decreases with neutralization of acid residues. For example, the dipole moment for the mutant *fld*$^{+6}$ was only half that of wild type (190 *vs* 381 D, respectively). However, somewhat surprisingly, the origin and direction of the dipoles do not change substantially. The negative end of the dipole vector is generally toward the FMN cofactor, at an angle of about 30° to the plane of the flavin isoalloxazine ring. The dipole moment for cytochrome c_3 is substantially lower than for the wild-type flavodoxin (84 D), with the positive end of the dipole moment vector oriented approximately through the plane of heme 4 rather than heme 1. This is noteworthy in that heme 1 is surrounded by the most basic surface and is the heme group at the interface of the modeled flavodoxin−cytochrome c_3 complex. The orientation of the dipole moment may be explained by the fact that the surface electrostatic potential map (Stewart *et al*., 1988) shows that three out of four hemes have a net positively charged environment, while that for heme 2 is negative.

DISCUSSION

This study was initiated to investigate the validity and functionality of the hypothetical molecular model for the electron transfer complex between the flavodoxin and cytochrome c_3 from *D. vulgaris* as described by Stewart *et al.* (1988). In that model, several acidic residues surrounding the FMN binding site of the flavodoxin are proposed to ion-pair with complementary lysine residues surrounding heme 1 of the cytochrome. As an electron transfer complex, this graphical complex seems particularly attractive because these pairings result in the coplanar alignment of the flavin and heme ring systems within van der Waals contact of one another, a situation seemingly ideal for efficient electron transfer. A similar graphical model has been proposed more recently for the binary and a possible ternary complex between the *D. gigas* cytochrome c_3 and the flavodoxin from *D. salexigens* (Palma *et al*., 1994).

The electron transfer kinetics between reduced cytochrome c_3 and each of a total of 17 mutants of the flavodoxin from *D. vulgaris* were established by stopped-flow spectrophotometry. These flavodoxin mutants include those in which each of 10 acidic amino acid residues were permanently neutralized, either individually or in various multiple combinations through the substitution of the corresponding amide analogue for each acidic residue using standard site-directed mutagenesis technology; *e.g.*, asparagine was substituted for aspartic acid. Among the singly neutralized mutants, small differences in both k_{lim} and K_{app} were noted between the group of residues included in the modeled complex and those that are not. Much larger differences were noted for several of the flavodoxin mutants in which more than one acidic residue was permanently neutralized. It is perhaps not surprising that the individual neutralization of acidic residues involved in complex formation does not have as large an effect on k_{lim} as the multiple mutations. If multiple ion-pairing interactions are involved in the formation of the initial complex, each ion pair would be contributing a fraction of the total binding energy. While all possible combinations were not studied for practical reasons, the data are nonetheless quite consistent with the model; that is, multiple mutations involving more than one complex-forming residue always generated a large increase in k_{lim} while the neutralization of residues not involved in complex formation, either in combination with others in this group or with complex-forming residues, had little effect. Because of the larger changes in k_{lim} associated with the multiple mutations, these results provide more convincing support for Asp62, Glu66, and Asp95 playing an important role in electron transfer while Asp63, Glu99, and Asp106 do not. Multiple mutations involving Asp69 and Asp129 were not available for this study and the results from the neutralization of these residues individually were rather inconclusive, so less proof is available for their participation in complex formation as proposed. Ideally, one might have liked to test the effects of the simultaneous neutralization of all five acidic residues in the modeled complex; however, based on the trends observed for those mutants reported here, the rates of electron transfer would have been much too fast to determine by conventional stopped-flow spectrophotometry. For this reason, the considerable effort to produce and characterize this mutant was not undertaken.

While implicating the involvement of several acidic residues in electron transfer, this study produced results that were seemingly counterintuitive to those expected on the basis of a simple bimolecular model for electron transfer between cytochrome c_3 and flavodoxin involving an intermediary complex stabilized by electrostatic interactions. In such an electron transfer mechanism, one might anticipate that the irreversible neutralization of acidic residues critical for the formation of ion pairs at the interface of the complex would result in higher K_{app} values and possibly lower electron transfer rates. This did not seem to be the case, however. With the exception of Asp95, Glu99, and Asp106 neutralizations, the K_{app} values for all singly neutralized mutants are all somewhat higher than for wild type. The neutralizations of Glu99 and Asp106, two residues not included in the modeled complex, result in K_{app} values close to that for wild type, as might be expected, but this trend does not hold for the other singly neutralized mutants involving residues not included in the complex. The neutralization of Asp95 generates the most pronounced effects on both k_{lim} and K_{app} of the singly neutralized mutants. While not completely understood, this phenomenon could be explained by the close proximity of this residue to the FMN cofactor. In fact, the main-chain atoms of this residue interact directly with the N1/C2O atoms of the flavin. If Asp95 is forming part of the interface between these proteins in the electron transfer complex, it is conceivable that changes in the properties of the FMN could be induced, resulting in the larger effects of the Asp95 to asparagine substitution.

Because electron transfer reaction can be affected by many factors, further kinetic studies were conducted to gain greater insight into this process. Though we cannot derive a certain mechanism for an electron transfer reaction, based on kinetic studies, we still can eliminate some mechanisms and develop a minimal mechanism as follows. Results of all flavodoxin mutants at different temperatures and ionic strengths showed that observed rates reached maximum values at high flavodoxin concentrations. This indicates the formation of complex occurs prior to the electron transfer leading to the minimal mechanism

$$\mathrm{Fld_{ox}} + \mathrm{Cyt_{red}} \underset{k_{-1}}{\overset{k_1}{\rightleftharpoons}} \mathrm{Fld_{ox}{\cdot}Cyt_{red}} \xrightarrow{k_{et}} \mathrm{Fld_{red}{\cdot}Cyt_{ox}}$$

At high flavodoxin concentrations, the observed rate constant should converge to maximum value, which is equal to k_{et}. However, the kinetic results demonstrated that the limiting observed rate constants could be as low as 30 s^{-1} at 25 °C or as high as 600 s^{-1} at 10 °C for different flavodoxin mutants. These rate constants are substantially lower than anticipated if actual electron transfer were rate-limiting, which by use of the Marcus equation can be estimated to be at least *ca.* 10^7 s^{-1} for the modeled complex.[3] Thus, given the nature of the amino acid substitutions involved and the relatively slow transfer rates, it is very unlikely that the maximum observed rate constants actually represent k_{et}. Instead, other events must limit electron transfer, suggesting a more complex mechanism of the type

$$\mathrm{Fld_{ox}} + \mathrm{Cyt_{red}} \underset{k_{-1}}{\overset{k_1}{\rightleftharpoons}} \mathrm{Fld_{ox}{\cdot}Cyt_{red}} \underset{k_{-2}}{\overset{k_2}{\rightleftharpoons}} \mathrm{Fld_{ox}{\cdot}Cyt_{red}}^{*} \xrightarrow{k_{et}} \mathrm{Fld_{red}{\cdot}Cyt_{ox}}$$

In this mechanism, after the initial formation of the complex, there is a reorganization step prior to electron transfer. Based upon a steady-state approximation and under pseudo-first-order conditions with flavodoxin in excess, k_{obs} can be represented as (Bendell, 1996)

$$k_{obs} = k_1 k_2 k_{et}[\mathrm{Fld}]/\{k_{-1}(k_{et} + k_{-2}) + k_2 k_{et} + k_1(k_{et} + k_2 + k_{-2})[\mathrm{Fld}]\}$$

The following relationships can also be derived:

$$k_{lim} = k_2 k_{et}/(k_2 + k_{-2} + k_{et})$$

and

$$K_{app} = \{k_{-1}(k_{et} + k_{-2}) + k_2 k_{et}\}/\{k_1(k_{et} + k_2 + k_{-2})\}$$

Several assumptions can be made to simplify the kinetic equations leading to the following electron transfer situations [terminology from Davidson (1996)]. In all cases, the formation of the initial complex was assumed to be in rapid equilibrium such that k_1 and k_{-1} are much larger than the limiting rate. This assumption is supported by the absence of any noticeable lag phase in the electron transfer reactions, by the saturation behavior, and by the fact that successful encounters between the two proteins could occur near the diffusion limit. Also, the electron transfer reaction was assumed to be irreversible given the substantial differences between the midpoint potentials of the donor and acceptor (Bendall, 1996).

(1) True electron transfer: The observed rate is limited by k_{et} only such that k_2, $k_{-2} \gg k_{et}$ and $K_2 \gg 1$. The reorganization step greatly favors the formation of electron transfer efficient complex and the mechanism degenerates to the simple binding mechanism in which the reorganization step is not observable. This situation is unlikely because, as discussed previously, k_{lim} should be similar for all mutants and the observed electron transfer rates are much slower than predicted for this complex.

(2) Coupled electron transfer: The observed rate is limited by both K_2 and k_{et}. Here again, the reorganization step should also be in rapid equilibrium, *i.e.*, k_2, $k_{-2} \gg k_{et}$ and K_2 is not substantially larger than 1. In this case, $k_{lim} = k_2 k_{et}/(k_2 + k_{-2})$ and $K_{app} = K_d k_2/(k_2 + k_{-2})$. In comparing the kinetic data for the mutants to that for wild type, the change in k_{lim} results from a change in $k_2/(k_2 + k_{-2})$. The change in K_{app} is also caused by a change in $k_2/(k_2 + k_{-2})$, as well as changes in K_d, which normally increases in mutants. According to this situation, when k_{lim} increases for the different mutants, K_{app} should increase by at least the same amount. But that is not in agreement with our results.

(3) Gated electron transfer: The observed rate is limited by K_2 only; *i.e.*, $k_2 \ll k_{et}$. In this situation, $k_{lim} = k_2 k_{et}/(k_{-2} + k_{et})$ and $K_{app} = K_d k_{et}/(k_{-2} + k_{et})$. As in the coupled

[3] A *nominal* electron transfer rate for the modeled electron transfer complex was calculated using the Marcus equation, $k_{et} = k_0 \exp\{-\beta(r - r_0)\}\exp\{[-(\Delta G_0 + \lambda)^2]/4\lambda RT\}$, and the following assumptions and values: $k_0 = 10^{13}$ s^{-1}, $\beta = 0.7-1.4$ Å^{-1}, $r = 6$ Å (nominal distance between the methyl groups of the FMN and the closest edge of the heme in the modeled complex), $r_0 = 3$ Å, $\Delta E_m \sim 150$ mV based on the oxidized/semiquinone couple of the wild-type flavodoxin and the average reported value for the heme groups of cytochrome c_3, $\lambda = 0.7-1.4$ eV, and $T = 283$ K.

mechanism, k_{lim} and K_{app} are both dependent on the kinetics of the reorganization step.

As a further test of the proposed mechanism, the kinetic simulation program KINSIM (Barshop *et al*., 1983) was used to simulate each of these three situations. Although the simulations could be made to fit all three mechanisms, the first two circumstances require the use of unrealistic values for several of the rate constants. For example, k_{et} must be set at unrealistically low values to satisfy the true electron transfer mechanism, and the observed changes in K_{app} for the group of mutants cannot be simulated according to the coupled mechanism. Only the last situation, the gated electron transfer mechanism in which the observed rate is limited by K_2, satisfactorily conforms to the experimental results and adequately explains why different mutants have different k_{lim} and K_{app} values. Based on this kinetic mechanism, the electron transfer reaction can be envisioned as follows.

First, as cytochrome c_3 and flavodoxin approach one another in solution, they may begin to orient themselves to one another through the interaction of their general electrostatic fields as is represented by the macromolecular dipole moment vectors shown in Figure 6. However, although the charge neutralizations introduced in the flavodoxin did reduce the magnitude of this dipole moment, its direction was not significantly affected. It is unclear for our data how important this "steering" process might be in the formation of this electron transfer complex. Nonetheless, the two proteins ultimately form a relatively stable initial complex involving several salt linkages between lysine residues on the cytochrome and several acidic residues on the flavodoxin. Our data suggest that these residues include at least three of those included in the modeled complex proposed by Stewart *et al.* (1988) although, with the exception of E99 and D106, all the acidic residues involved in this study generally form a negatively charged "ring" around FMN, which could form an interface within this complex. It is not possible to determine the structure of this initial complex as well as the ion pairing involved at this point. It is plausible that it is different from the modeled complex, especially since that complex brings the two redox centers into van der Waals contact, a configuration seemingly optimal for electron transfer. It is also likely that this initial complex is a mixture of several different configurations involving these residues. Regardless, our kinetic data suggest that this complex is either inactive or very inefficient in terms of electron transfer. This initial complex undergoes a slow rearrangement or reorganization involving the disruption of one or more of the initial salt linkages to form an active electron transfer complex, perhaps forming the complex proposed by Stewart *et al.* (1988). The neutralization of one or more of the acidic residues involved in the initial complex disrupts these ion pairs, weakening the electrostatic interactions in the initial complex. This situation favors the rearrangement of the complex by increasing k_2, which is a rate-limiting step in this mechanism. By increasing k_2 and decreasing k_{-2}, the overall observed electron transfer rate is increased as observed for several of the mutants. Also, neutralization weakens the initial complex formation and K_d is increased. That affects the change of K_{app}, but the magnitude of change is not as great as that of k_2, again consistent with the kinetic data. This effect is even more distinctive in mutants containing multiple acid-to-amide substitutions. The larger the number of neutralization of acidic residues involved in the complex formation, the weaker the electrostatic interaction and the faster the overall electron transfer rate. Also, the fact that in this mechanism k_2 is rate-limiting is consistent with the absence of a correlation between the observed electron transfer rate and the midpoint potential for the ox/sq couple (Figure 4). Changes in midpoint potential should primarily affect k_{et}.

Further evidence for this mechanism was provided by ionic strength dependency of the observed electron transfer rates as shown in Figure 5. Several distinct characteristics were observed and can be explained within the context of the proposed mechanism as follows. First, at low ionic strength, rates increased as the ionic strength of the solution was increased. This is likely the result of the increased strength of the electrostatic interactions at low ionic strength, "locking in" the initial inactive or inefficient complex. Thus, at low ionic strength it would be more difficult for this complex to reorganize into the active electron transfer complex. Increasing the ionic strength facilitates the rearrangement of the initial complex, in effect, increasing K_2 and increasing the observed electron transfer rate as observed. After the ionic strength reaches a certain threshold, the rates begin to decrease again due to the weakening of the electrostatic interactions in both the productive and nonproductive complexes. Because the wild-type flavodoxin has potentially a larger number of acidic residues participating in complex formation, a broader ascending range is expected, as observed. For the same reason, the electrostatic interactions in wild-type complex are expected to be stronger than that of *fld*$^{+5}$ mutant, requiring a higher ionic strength to destabilize the initial complex. This multiphasic behavior is similar to that described for other electron transfer systems including the nonphysiological complexes between *c*-type cytochromes and plastocyanin (Meyer *et al*., 1993) and the more physiological complexes involving ferredoxin and ferredoxin:NADP$^+$ reductase (Hurley *et al*., 1996) as well as cytochrome *c* and cytochrome *c* oxidase (Hazzard *et al*., 1991). The trend in which transfer rates increase with decreasing ionic strength has also been described for electron transfer between *c*-type cytochromes and various flavodoxins (Simondsen *et al*., 1982; Cheddar *et al*., 1986); however, measurements were not performed at ionic strengths below 40 mM, where the rates begin to fall off in those cases.

Recently, Watkins *et al*. (1994) have developed a theoretical model that attempts to describe the effect of ionic strength on the bimolecular rate constant for interprotein electron transfer. This model averages the dielectric constant and dipole moment for the area of intermolecular contact and simplifies the interface region between the two proteins to a uniformly charged "parallel plate". We have also attempted to fit our data with this parallel plate model. Both monopole−monopole and dipole−monopole interactions are included in our calculations. Dipole−dipole interactions were not included because in the modeled complex the relative orientation of the macromolecular dipole moments of each protein is approximately 90°, a point at which this contribution is negligible (Watkins *et al*., 1994). The ionic strength dependency of both the wild-type and *fld*$^{+5}$ mutant can be adequately fit to the model at both low and high ionic strength as shown in Figure 5. However, the monopole (V_{ii}) and dipole (V_{id}) terms are of opposite signs, which is physically unreasonable (Watkins *et al*., 1994). This dis-

crepancy is apparently due to the complexity of the electron transfer mechanism at low ionic strength where the strong electrostatic interaction locks the initial complex and disfavors the electron transfer. Such a phenomenon has been noted in other electron transfer systems (*e.g.*, Cheddar *et al*., 1989; Meyer *et al*., 1993; Watkins *et al*., 1994). However, the descending limb of the dependency can be described reasonably well by the parallel plate model when including only monopole−monopole or both monopole−monopole and dipole−monopole interactions in the fitting process. The parameters obtained from such fits (included in Figure 5) indicate that more charges were involved in forming the electron transfer complex for wild-type flavodoxin than for the *fld*$^{+5}$ mutant and consequently the diameter of "parallel plate" interface (ρ) for wild type is larger than that for *fld*$^{+5}$. These results are consistent with the role of electrostatic interactions in forming the electron transfer complex between flavodoxin and cytochrome c_3 and support the functional importance of at least some of the acidic residues neutralized in that mutant. It is also interesting to note that, for all of the fitting procedures, similar second-order rate constants were obtained at infinite ionic strength ($\sim 4.4 \times 10^5$ M^{-1} s^{-1}), a condition in which ion-pairing interactions are negligible, providing further support for our conclusions that the changes in the electron transfer rates observed for this group of flavodoxin mutants are the consequence of alterations in the electrostatic interactions rather than of changes in the intrinsic electron transfer rate (k_{et}) itself.

In some protein−protein complexes involving cytochrome c_3, heme 1 is most likely to be in the interface (Guerlesquin *et al*., 1994). It is surprising that the dipole moment of cytochrome c_3 does not direct toward heme 1 but toward heme 4. Even though heme 1 is surrounded by a group of lysine residues and has the most electrostatic positive environment, heme 4 is also surrounded by some lysine groups and the molecular surface is positively charged. Considering the midpoint potential difference and the strength of dipole−dipole interaction, heme 1 is more likely to transfer its electron to the FMN. But a possibility still exists that electron transfer could occur between the flavodoxin and heme 4. Kinetics results show a fast phase and a slow phase, which was demonstrated previously to be due to two different cytochrome c_3 conformations (Moura *et al*., 1982). Biphasic behavior can also result from the presence of two different binding sites on the cytochrome, one of which leads to more efficient electron transfer than the other. Further study needs to be done to elucidate more completely the binding sites on cytochrome c_3.

In conclusion, the results obtained from the study of this group of acid-to-amide charge-neutralized flavodoxin mutants support portions of the graphical model of the electron transfer complex between flavodoxin and cytochrome c_3 proposed by Stewart *et al.* (1988). The kinetic data strongly implicate Asp62, Glu66, and Asp95 as influential acid residues in the formation of electrostatic interactions that control electron transfer as proposed in that model. However, our data suggest that the ion pairing may initially lead to a complex in which electron transfer is relatively inefficient. Weakening the initial binding at low ionic strength could enhance the electron transfer, presumably by allowing for the rapid reorganization of the complex after the initial complex is formed, largely through longer-range electrostatic interactions. It is not possible to determine whether the modeled complex represents the optimal configuration for electron transfer obtained after the reorganization step or actually represents the initial complex. Our data do provide evidence for the existence of alternative binding sites or modes involving acidic residues on the surface of the flavodoxin other than those proposed by Stewart *et al.* (1988). Finally, these results seemingly raise an interesting apparent paradox. The five acidic residues proposed to ion-pair in this electron transfer complex are highly conserved in the flavodoxins characterized from several members of the *Desulfovibrio* family (Helms, 1990). Some such as Glu66, Asp69, and Asp95 are always present as an acidic residue; others are conserved in at least four of the flavodoxins. If electron transfer is actually impeded by the presence of several of these residues, why are they seemingly retained? One can only speculate. We know that the asymmetric distribution of acidic residues around the FMN cofactor is a major determinant of the midpoint potential of the flavin, especially for the semiquinone/hydroquinone couple, and they may be conserved for this purpose (Zhou & Swenson, 1995). It is also plausible that within the cell the ionic strength may reduce some of the inhibitory effects of the initial electrostatic interactions as demonstrated in Figure 5. Also, it is highly likely that flavodoxins participate in many electron transfer reactions involving several redox partners. Perhaps the participation of the surface residues represents a compromise among several different types of electron transfer complexes that must be formed by the flavodoxin molecule *in vivo*.

ACKNOWLEDGMENT

We acknowledge the considerable efforts of Dr. Zhimin Zhou who, for other studies, prepared many of the flavodoxin mutants used in this work and Dr. Mesut Eren for providing the initial cellular extract from *D. vulgaris* from which the cytochrome c_3 was purified.

REFERENCES

Badziong, W., & Thauer, R. K. (1980) *Arch. Microbiol. 125*, 167−174.

Barata, B. A., LeGall, J., & Moura, J. J. (1993) *Biochemistry 32*, 11559−11568.

Barshop, B. A., Wrenn, R. F., & Frieden, C. (1983) *Anal. Biochem. 130*, 134−145.

Bendall, D. S. (1996) in *Protein Electron Transfer* (Bendall, D. S., Ed.) pp 43−68, BIOS Scientific Publishers Ltd., Oxford, England.

Cheddar, G., Meyer, T. E., Cusanovich, M. A., Stout, C. D., & Tollin, G. (1986) *Biochemistry 25*, 6502−6507.

Cheddar, G., Meyer, T. E., Cusanovich, M. A., Stout, C. D., & Tollin, G. (1989) *Biochemistry 28*, 6318−6322.

Chen, L., Liu, M. Y., & LeGall, J. (1993) *Arch. Biochem. Biophys. 303*, 44−50.

Curley, G. P., Carr, M. C., Mayhew, S. G., & Voordouw, G. (1991) *Eur. J. Biochem. 202*, 1091−1100.

Davidson, V. L. (1996) *Biochemistry 35*, 14035−14039.

De Francesco, R., Edmondson, D. E., Moura, I., Moura, J. J. G., & LeGall, J. (1994) *Biochemistry 33*, 10386−10392.

Fujisawa, H., & Hayaishi, O. (1968) *J. Biol. Chem. 243*, 2673−2681.

Guerlesquin, F., Dolla, A., & Bruschi, M. (1994) *Biochimie 76*, 515−523.

Hazzard, J. T., Rong, S., & Tollin, G. (1991) *Biochemistry 30*, 213−222.

Helms, L. R. (1990) Ph.D. Thesis, The Ohio State University, Columbus, OH.

Higuchi, Y., Kusunoki, M., Matsuura, Y., Yasoka, N., & Kakudo, M. (1984) *J. Mol. Biol. 172*, 109−139.
Hurley, J. K., Schmeitz, J. L., Genzor, C., Gómez-Moreno, C., & Tollin, G. (1996) *Arch. Biochem. Biophys. 333*, 243−250.
Koppenol, W. H., & Margoliash, E. (1982) *J. Biol. Chem. 257*, 4426−4437.
Krey, G. D., Vanin, E. F., & Swenson, R. P. (1988) *J. Biol. Chem. 263*, 15436−15443.
Kunkel, T. A. (1985) *Proc. Natl. Acad. Sci. U.S.A. 82*, 488−492.
Liu, M.-C., Costa, C., Coutinho, I. B., Moura, J. J. G., Moura, I., Xavier, A. V., & LeGall, J. (1988) *J. Bacteriol. 170*, 5545−5551.
Marcus, R. A., & Sutin, N. (1985) *Biochim. Biophys. Acta 811*, 265−322.
Margoliash, E., & Bossard, H. R. (1983) *Trends Biochem. Sci. 8*, 316−320.
Mazin, A. L., Sulimova, G. E., & Vanyushin, B. F. (1974) *Anal. Biochem. 61*, 62−71.
Meyer, T. E., Zhao, Z. G., Cusanovich, M. A., & Tollin, G. (1993) *Biochemistry 23*, 4552−4559.
Moreno, M., Campos, A., Teixeira, M., LeGall, J., Montenegro, M. I., Moura, I., van Dijk, C., & Moura, J. J. G. (1991) *Eur. J. Biochem. 202*, 385−393.
Moura, J. J. G., Xavier, A. V., Hatchikian, D. C., & LeGall, J. (1978) *FEBS Lett. 89*, 177−179.
Moura, J. J. G., Santos, H., Moura, I., & LeGall, J. (1982) *Eur. J. Biochem. 127*, 151−155.
Moura, J. J. G., LeGall, J., & Xavier, A. V. (1984) *Eur. J. Biochem. 141*, 319−322.
Nicholls, A., & Honig, B. (1991) *J. Comput. Chem. 12*, 435−445.
Palma, P. N., Moura, I., LeGall, J., Van Beeumen, J., Wampler, J. E., & Moura, J. J. (1994) *Biochemistry 33*, 6394−6407.
Pelletier, H., & Kraut, J. (1992) *Science 258*, 1748−1755.
Roberts, V. A., Freeman, H. C., Olson, A. J., Tainer, J. A., & Getzoff, E. D. (1991) *J. Biol. Chem. 266*, 13431−13441.
Sanger, F., Nicklen, S., & Coulson, A. R. (1977) *Proc. Natl. Acad. Sci. U.S.A. 74*, 5463−5467.
Simondson, R. P., Weber, P. C., Salemme, F. R., & Tollin, G. (1982) *Biochemistry 21*, 6366−6375.
Stewart, D. E., LeGall, J., Moura, I., Moura, J. J. G., Peck, H. D., Jr., Xavier, A. V., Weiner, P. K., & Wampler, J. E. (1988) *Biochemistry 27*, 2444−2450.
Swenson, R. P., & Krey, G. D. (1994) *Biochemistry 33*, 8505−8514.
Watkins, J. A., Cusanovich, M. A., Meyer, T. E., & Tollin, G. (1994) *Protein Sci. 3*, 2104−2114.
Weber, P. C., & Tollin, G. (1985) *J. Biol. Chem. 260*, 5568−5573.
Weiner, S. J., Kollman, P. A., Case, D. A., Singh, U. C., Ghio, C., Alagona, G., Profeta, S., Jr., & Weiner, P. (1984) *J. Am. Chem. Soc. 106*, 765−784.
Zhou, Z., & Swenson, R. P. (1995) *Biochemistry 34*, 3183−3192.

BI971576C